Coatings **2015**, *5*, 465-476; doi:10.3390/coatings5030465

OPEN ACCESS

coatings

ISSN 2079-6412

www.mdpi.com/journal/coatings

Article

Evaluation of Photocatalytic Properties of Portland Cement Blended with Titanium Oxynitride ($TiO_{2-x}N_y$) Nanoparticles

Juan D. Cohen [1], G. Sierra-Gallego [2] and Jorge I. Tobón [1,*]

[1] Grupo del Cemento y Materiales de Construción CEMATCO, Universidad Nacional de Colombia, Facultad de Minas, 05001000 Medellín, Colombia; E-Mail: jdcohenr@unal.edu.co

[2] Grupo Investigación en catálisis y nano materiales, Universidad Nacional de Colombia, Facultad de Minas, 05001000 Medellín, Colombia; E-Mail: geralsierraga@unal.edu.co

* Author to whom correspondence should be addressed; E-Mail: jitobon@unal.edu.co; Tel.: +57-318-404-3431.

Academic Editor: Anibal Maury-Ramirez

Received: 1 April 2015 / Accepted: 24 July 2015 / Published: 31 July 2015

Abstract: Photocatalytic activity of Portland cement pastes blended with nanoparticles of titanium oxynitride ($TiO_{2-x}N_y$) was studied. Samples with different percentages of $TiO_{2-x}N_y$ (0.0%, 0.5%, 1%, 3%) and TiO_2 (1%, 3%) were evaluated in order to study their self-cleaning properties. The presence of nitrogen in the tetragonal structure of TiO_2 was evidenced by X-ray diffraction (XRD) as a shift of the peaks in the 2θ axis. The samples were prepared with a water/cement ratio of 0.5 and a concentration of Rhodamine B of 0.5 g/L. After 65 h of curing time, the samples were irradiated with UV lamps to evaluate the reduction of the pigment. The color analysis was carried out using a Spectrometer UV/Vis measuring the coordinates CIE (Commission Internationale de l'Eclairage) L^*, a^*, b^*, and with special attention to the reddish tones (Rhodamine B color) which correspond to a^* values greater than zero. Additionally, samples with 0.5%, 1%, 3% of $TiO_{2-x}N_y$ and 1%, 3% of TiO_2 were evaluated under visible light with the purpose of determining the Rhodamine B abatement to wavelengths greater than 400 nm. The results have shown a similar behavior for both additions under UV light irradiation, with 3% being the addition with the highest photocatalytic efficiency obtained. However, $TiO_{2-x}N_y$ showed activity under irradiation with visible light, unlike TiO_2, which can only be activated under UV light.

Keywords: photocatalysis heterogeneous; Portland cement; self-cleaning; nanoparticles of titanium oxynitride ($TiO_{2-x}N_y$); degradation of rhodamine B; UV light

1. Introduction

Nanotechnology has become a very important research topic in recent years for the scope and variety of applications in almost all fields of engineering. Mainly though, it has been important in the development of new materials. For example, nanotechnology has been implemented in the study of building materials in order to improve the mechanical properties and give the materials other additional properties. In these studies, the addition of carbon nanotubes to reduce fissures and improve mechanical properties [1], as well as the insertion of nanoparticles of silica (n-SiO_2) [2] and iron oxide (Fe_2O_3) for the sealing of nanopores [3] has been highlighted. Other types of features have been given to cement, when broadband semiconductor nanoparticles are added, such as the decontaminating of air, and the self-cleaning in buildings, through photocatalytic activity [4]. These properties are obtained, for example, when photocatalytic reactions are performed in the nanoparticles interface incorporated in the cementitious matrices. These reactions are defined as electrochemical processes by absorption of radiant energy (UV light) within the photocatalyst, which is usually a semiconductor with broadband [5]. When photons of a required wavelength (photons with energy higher than the band gap of the photocatalyst), are absorbed by the photocatalyst, electrons from the valence band are promoted to the conduction band crossing through the band gap (forbidden region for electronic states), and electron-hole pairs are generated. These pairings carry opposed free charges in the absence of an electric field, and recombine rapidly (in approximately of 30 ns), releasing excess energy, mainly as heat [6]. If there are previously adsorbed chemical species in the catalyst surface, recombination is prevented and redox reactions occur between these species and the photogenerated pairs. In this case, the electrons (−) react with oxidizing agents, and the holes (+) react with reducing agents. Photocatalysis is normally effected under aerobic conditions, (when oxygen acts as an acceptor species) and will react with the electrons (e^-) to form a superoxide radicals ($O_2^{\bullet -}$). In turn, the water is used as a reducing agent, and it will react with the holes (h^+) to form hydroxyl radicals ($OH^\bullet$) [5]. The following Equations (1)–(3) correspond to the reactions carried out in the photocatalyst interface:

$$TiO_2 + hv \rightarrow TiO_2(e^- + h^+) \quad (1)$$

$$TiO_2(h^+) + H_2O \text{ ad.} \rightarrow TiO_2 + OH^\bullet \text{ad} + H^+) \quad (2)$$

$$TiO_2\ (e^-) + O_2 \rightarrow TiO_2 + O_2^{\bullet -} \quad (3)$$

Studies with photocatalytic cements have been performed mostly by adding TiO_2 nanoparticles, and UV radiation as a photon source. The use of TiO_2 is due to its low toxicity and high stability compared to other semiconductors studied for this application (ZnO, CdS, WO_3) [6]. The NO_x abatement has been evaluated for cement pastes added with TiO_2 nanoparticles at different ratios of rutile and anatase [7]. In this same way, there has been reported the mineralization of different VOCs (Volatile Organic Compounds) by means of building materials added with TiO_2 [8]. The self-cleaning ability in these kind of cements is evaluated by standard UNI 11259, using Rhodamine B as an organic dye. In this case,

important results have been obtained with mortars and cement pastes, using TiO_2 as addition [9–11]. The Rhodamine B is selected for evaluating this property in cements, mainly because it is very soluble in water, its discoloration can be followed by colorimetry and it has little sensitivity to the alkalinity of cementitious materials [10]. Additionally, the rhodamine B has polycyclic aromatic hydrocarbons in its chemical structure, compounds that are usually found as pollutants in urban environments. On the other hand, it is known that the main weakness of these cements is given by the nature of TiO_2, which is only activated in the presence of UV light. The wavelengths in the UV region of the solar spectrum correspond to a low percentage and, thus, there is minimal use of stimulus of light when implementing these cements into a real life scenario. An alternative though, according to the research performed by Asahi, is to modify the photocatalyst with impurities to improve the efficiency of the process. This research found that the presence of nitrogen in the structure of TiO_2 as substitution by oxygen creates Ti–N bonds and electronic states in forbidden energy levels [12,13]. This anionic partial substitution increases the range of the solar spectrum absorbed [14]. In this case, nanoparticles of TiO_xN_y can absorb wavelengths between 365 nm and 500 nm [15,16]. An approach of the behavior of these nanoparticles in building materials was done by mixing nano-$TiO_{2-x}N_y$ with calcium carbonate ($CaCO_3$). This blend reduced the concentration of NO_x and 2-propanol between 360 and 436 nm [17]. The addition of nano-$TiO_{2-x}N_y$ to the cement is entirely unknown; therefore, the main objective of this research is to discuss the behavior of these nanoparticles in the cement and obtain a construction material with a self-cleaning property in the presence of UV and visible light.

2. Experimental Section

2.1. Raw Materials

Samples were prepared using commercial Portland white cement type I from the Colombian company Cementos Argos. The Titanium Oxynitride ($TiO_{2-x}N_y$) and Titanium Dioxide (TiO_2), commercial references were provided by Chinese NaBond Technologies Co. (Shenzhen, China) and German companies Evonik-Degussa (Essen, Germany), respectively. In turn, according to the manufacturer, the $TiO_{2-x}N_y$ has 22% Nitrogen in its structure. The Rhodamine B was provided by the Colombian enterprise Codim. Table 1 shows the specifications of each nanoparticle and the crystalline phases and semi-quantitative estimations using X-ray diffraction (XRD, Phillips X'pert).

Table 1. Characteristics of nanoparticles added.

Sample	BET* (m^2/g)	Dv.50* (nm)	Crystalline phases (%) **
P25 (TiO_2)	50 ± 15	21	Anatase 87 Rutile 13
$TiO_{2-x}N_y$	31	30	Anatase 84 Rutile 16

*According to the manufacturer's specifications; ** Semi-quantitative estimation by XRD.

2.2. Preparation and Evaluation of the Samples

Samples were prepared into disc-shaped specimens of white cement paste with a 1.62 cm diameter and a 0.3 cm thickness. Deionized water was used for a water/cement ratio of 0.5. Previously, the nanoparticles were added in the mixed water and dispersed using a superplasticizer (Plastol HR-DF), provided by the company Toxement in Colombia. The dispersant agent was used with 19% by weight relative to the nanoparticles. Afterwards, this suspension was sonicated with 90 W and 35 kHz frequency (VWR® Symphony™ 97043-992) for 15 min [18]. Samples were prepared with three different percentages of cement content, for $TiO_{2-x}N_y$ 0.5%, 1%, 3%. Other samples were prepared with two levels of TiO_2, 1% and 3%. After, the samples were cured in a wet room for 65 h. Additionally, samples were prepared with 0.5%, 1%, 3% of $TiO_{2-x}N_y$, and another set with 1% and 3% of TiO_2, in order to evaluate the Rhodamine B abatement in visible light. Following the provisions of the standard [19], the pastes were immersed in water with Rhodamine B for one hour, at a concentration of 0.5 g/L in order to ensure a uniform color for each sample. The samples were irradiated with UV light using lamps emitting a wavelength spectrum between 350 and 400 nm (Phillips, Amsterdam, The Netherlands, Actinic BL TL-D(K), 30 W). In order to evaluate the behavior of the samples in visible light, a fluorescent lamp was used with a wavelength spectrum between 410 and 560 nm (Lite-Way, C13101, 24 W). The samples were irradiated to 20 $W/m^2 \pm 0.3$ for the UV experimental setup, as set out in the standard [19]. For the setup with visible light, the samples were irradiated to 10 $W/m^2 \pm 0.5$. For this setup, the height between the lamp and the samples was determined using a radiometer (PMA 2210, Solar Light Co., Philadelphia, PA, USA) coupled to a probe to detect wavelengths between 400 and 700 nm (LDC 21300, Solar Light Co., Philadelphia, PA, USA). To determine the color coordinates CIE (Commission Internationale de l'Eclairage) *L*a*b** [20], a UV/Vis Spectrometer was used (BWTEK Inc., Newark, NJ, USA, GlacierTM X, BTC112E), coupled with a probe for measuring reflection and backscatter (Ocean Optics, QR200-7-UV-VIS) and a support to hold it at 45° angle to the samples (Ocean Optics, Dunedin, FL, USA, RPH-1).

3. Results and Discussion

3.1. X-ray Diffraction (XRD)

Figure 1 corresponds to diffractograms of $TiO_{2-x}N$ and TiO_2, highlighting anatase and rutile phases. The shifting of peaks to the left is evidence of an enlargement of the unit cell, demonstrating the insertion of nitrogen atoms into the crystalline structure. Since the TiO_2 usually has oxygen vacancies that introduce localized states of Ti^{+3} [6], it is possible to insert some impurities that are compatible and dope the catalyst to improve performance. In this case, the nitrogen (N^{-3}) is likely to enter into the structure for having an atomic radius and electronegativity similar to O^{-2}. In this manner, the nitrogen supplies the anionic deficiency. Precisely, it is the nitrogen inserted in the interstices as a substitution of oxygen, which induces occupied electronic states on intervals known as the forbidden energy band (band gap) [13]. This process can facilitate the formation of electron-hole pairs, using stimuli such as electromagnetic radiation of wavelengths greater than 400 nm.

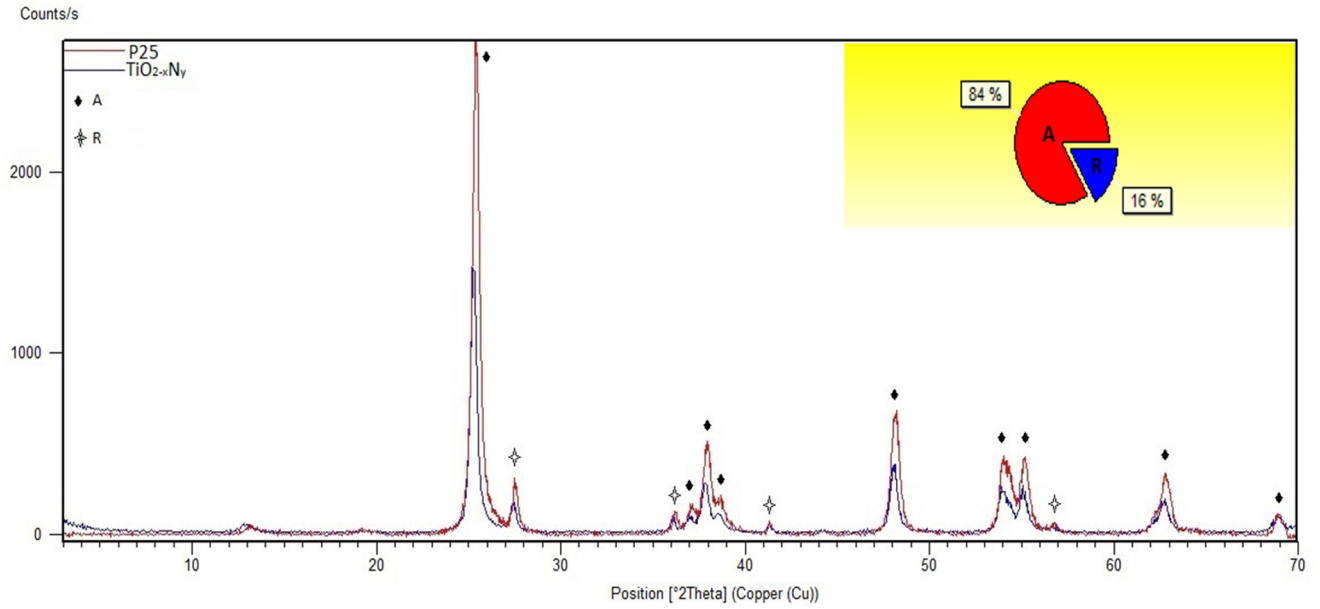

Figure 1. X-ray diffractogram (XRD) of Aeroxide P25 (TiO_2) *vs.* $TiO_{2-x}N_y$; phases anatase (A) and rutile (R).

3.2. Transmission Electron Microscope (TEM)

TEM images of nanoparticles of TiO_2 and $TiO_{2-x}N_y$, are reported in Figure 2. Both have almost the same distribution of phases, according to the diffractogram XRD viewed above. The anatase with a hexagonally shaped rounded, has a size about 20 nm (Figure 2a), while rutile shows a hexagonally shape and a size about 60 nm for TiO_2 (Figure 2a). In Figure 2b, $TiO_{2-x}N_y$ nanoparticles have an overall size of about 30 nm.

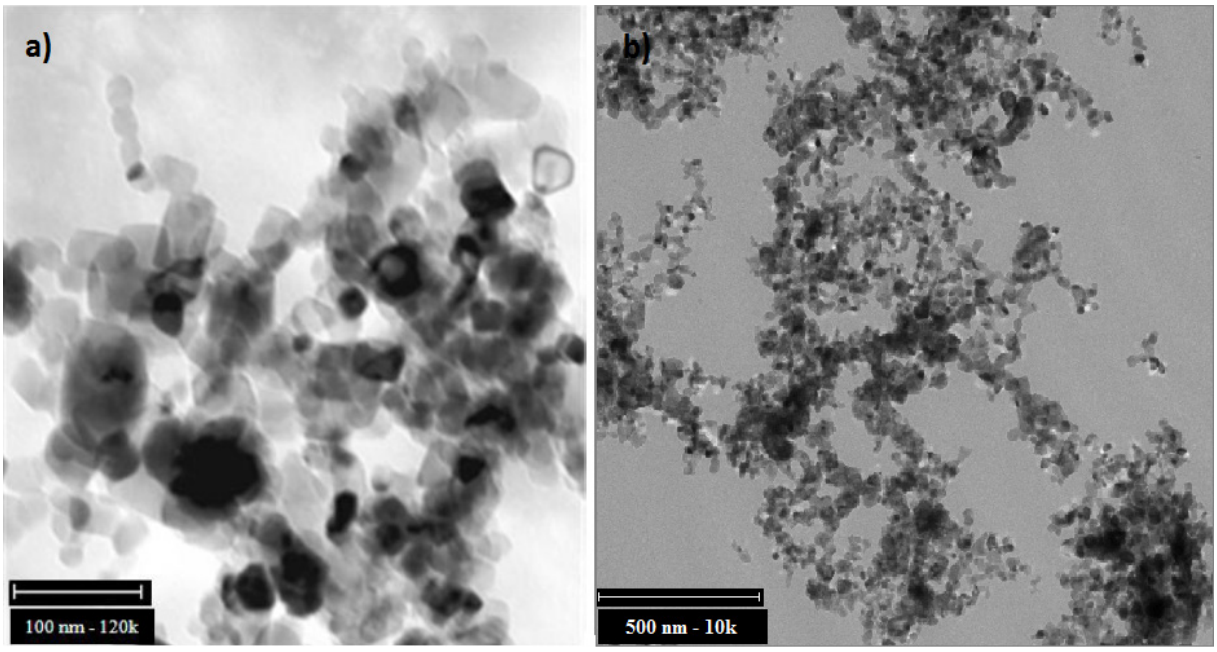

Figure 2. TEM images for nanopowders: (**a**) Aeroxide P25 (TiO_2) [11]; (**b**) $TiO_{2-x}N_y$ (NaBond Technologies Co., Shenzhen, China).

3.3. Abatement of Rhodamine B

The Rhodamine B degradation mechanism passes through two different pathways; the first being the deethylation process and the second being the destruction of the chromophore structure [21]. Such a dual mechanism seems to depend on the nature of the light in the photoinduction. Under UV-Vis conditions, there is no selectivity and the destruction of the chromophore is also involved during the degradation. [22]. Additionally, the results obtained during discoloration of the samples are observed in Figure 3, where Δa^* is defined as the change in coordinate a^* during the exposure time of the samples to UV light; being the initial hue at $t = 0$ and the final coordinate of the same sample at time t as shown below:

$$\Delta a^* = a_0^* - a_t^* \quad (4)$$

In this case, the coordinate a^* corresponds to a reddish hue for positive values, according the color-order system specified by the Commission Internationale de l'Eclairage [20]. The highest photoactivity was observed for samples with a 3% addition of $TiO_{2-x}N_y$ and TiO_2, as similarly reported by other works [10,11]. The control samples were also evaluated, to determine the catalytic reactions by photolysis or by temperature.

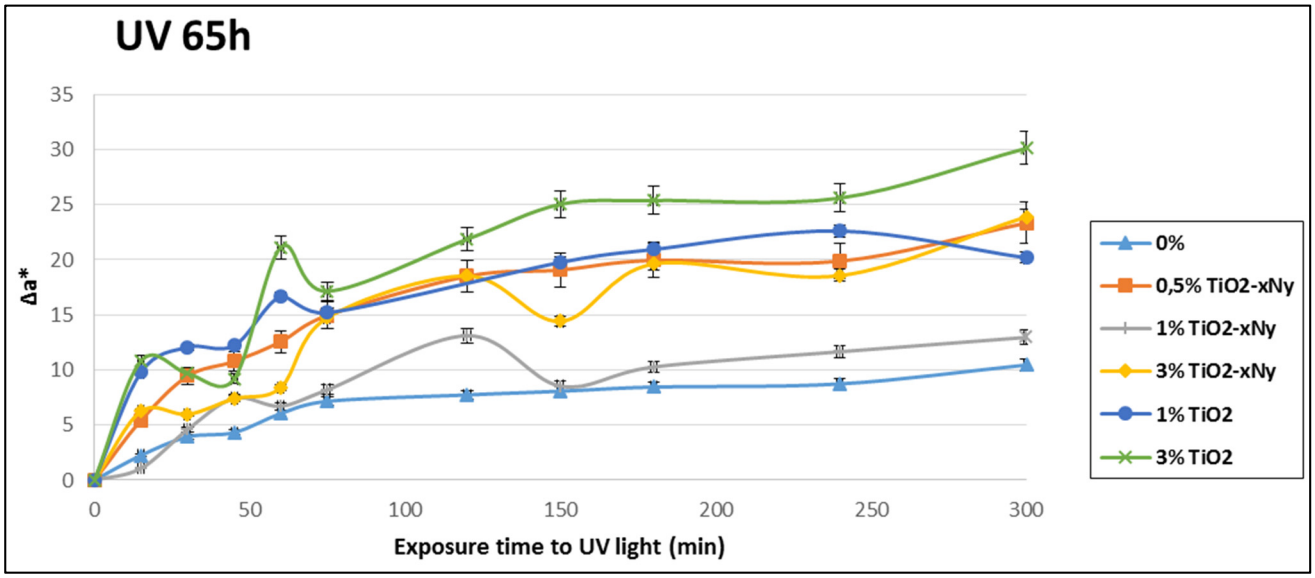

Figure 3. Change in Δa^* during five hour exposure to UV light with different addition percentages of $TiO_{2-x}N_y$ and TiO_2 for samples at 65 h of curing age.

There is a difference between the specimens with 3% of TiO_2 facing the other samples was observed, and the values of 0.5% of $TiO_{2-x}N_y$ were similar to the samples with 1% of TiO_2. It is noted that 0.5% of $TiO_{2-x}N_y$ showed a more significant change than 1% of $TiO_{2-x}N_y$; this behavior can be explained in two ways. The first explanation is that the action of the hydrated products forms a layer around nano- $TiO_{2-x}N_y$, which protects nanoparticles from abrasion and may decrease the photocatalytic activity [23]. Here, the nanoparticles act as nucleation sites in cement hydration increasing the accumulation of hydration products [24]. The second way is that the decrease in photocatalytic activity is explained by re-agglomeration of nanoparticles in the matrix of the cement as a consequence of low dispersion. This occurs also in the samples with 3% of $TiO_{2-x}N_y$, but the generation of active sites seems to be a more important factor in this case; therefore, the abatement of Rhodamine B is improved. Even

with this information, it is necessary to find other evidence, such as the generation of hydration products and the relationship of them with the content of nanoparticles in the cement and the photoactivity, in future works in order to ratify this hypothesis.

In order to determine a percentage of decrease of color, the photocatalytic efficiency coefficient (Ɛ) was calculated and is defined as:

$$\text{Ɛ} = \frac{A(a_0^*) - A(a^*)}{A(a_0^*)} \times 100 \quad (5)$$

where $A(a_0^*)$ corresponds to an ideal state in which the initial coordinate remains constant during t_f time, as established by Equation (6), and $A(a^*)$ the area under the real curve of a^*, as observed in Equation (7) [10].

$$A(a_0^*) = t_f \times a_0^* \quad (6)$$

$$A(a^*) = \int_{t_0}^{t_f} a^* \mathrm{d}t \quad (7)$$

Figure 4 shows the photocatalytic efficiency coefficients of the samples (cured 65 h) after 5 h of UV irradiation. Coefficients greater than those obtained for control samples (0%), are considered photocatalytic reactions and are products of the interaction between photons and the nanoparticles of photocatalyst. Otherwise, these coefficients are considered as other kinds of interactions, such as photolysis or thermolysis. It is noted, that all the additions showed photocatalytic activity and efficiency above the standard sample. In addition, a similar coefficient between the samples with 0.5% of $TiO_{2-x}N_y$ and 1% $TiO_{2-x}N_y$ was observed, different to results obtained in another research [11]. As explained above, this could be due to the re-aglomeration effect of the nanoparticles in the matrix cementitious. Similarly, a uniform performance of TiO_2 3% was observed for $TiO_{2-x}N_y$ 3%.

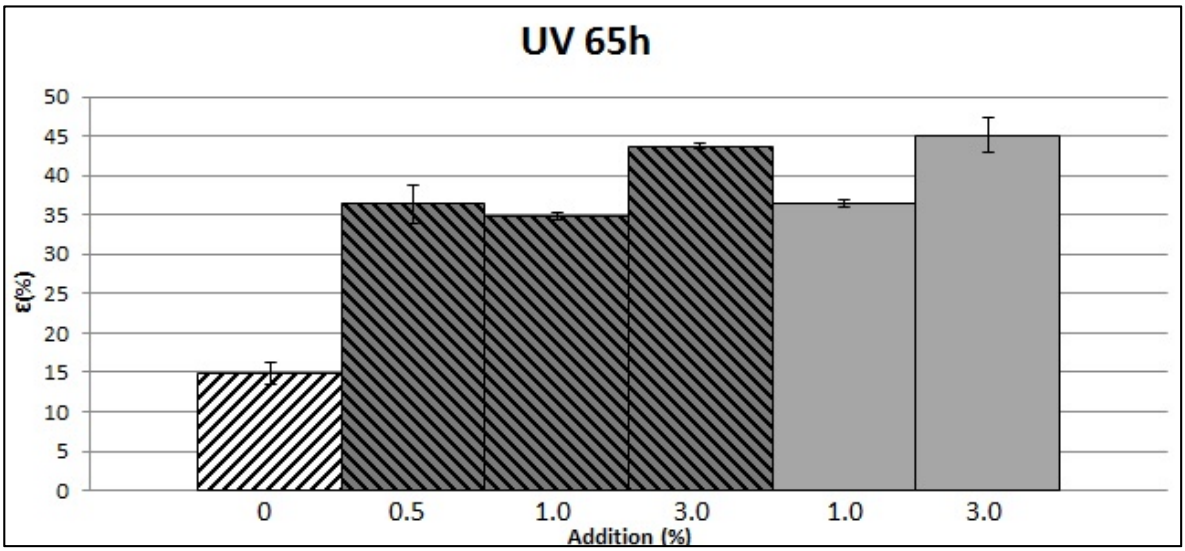

Figure 4. Photocatalytic efficiency Coefficient (ε) for samples in UV light with different addition percentages of $TiO_{2-x}N_y$ and TiO_2 for samples at 65 h of curing age, ▨ control sample, ▩ $TiO_{2-x}N_y$, ▭ TiO_2. Error bars are standard deviation.

Some samples were evaluated as well in visible light. In Figure 5, the comparison between samples of $TiO_{2-x}N_y$ with 0.5%, 1%, 3% and TiO_2 with 1%, 3% for the change in Δa^* *versus* exposure time is shown. It is noted that TiO_2 did not show photoactivity in visible light, mainly because of its wide band gap that only lets the electrons jump to the conduction band by stimuli of wavelengths below 400 nm.

Additionally, the photocatalytic efficiency coefficient for these samples was calculated. In Figure 6, the comparison between coefficients for samples with 0.5%, 1%, 3% of $TiO_{2-x}N_y$, and 1%, 3% of TiO_2, including control samples are reported. TiO_2 samples obtained values below the samples with 0%. The minimal change in a^* is attributed to other mechanisms, not to photocatalytic reactions. When percentages equal or below are obtained in comparison with the control sample (0%), there is no evidence of photocatalytic interactions; therefore, the change in hue is attributed to photolysis and thermolysis reactions. It is possible that TiO_2 nanoparticles create a shielding effect in the samples, blocking photonic absorption in the pigment and preventing photolysis reactions.

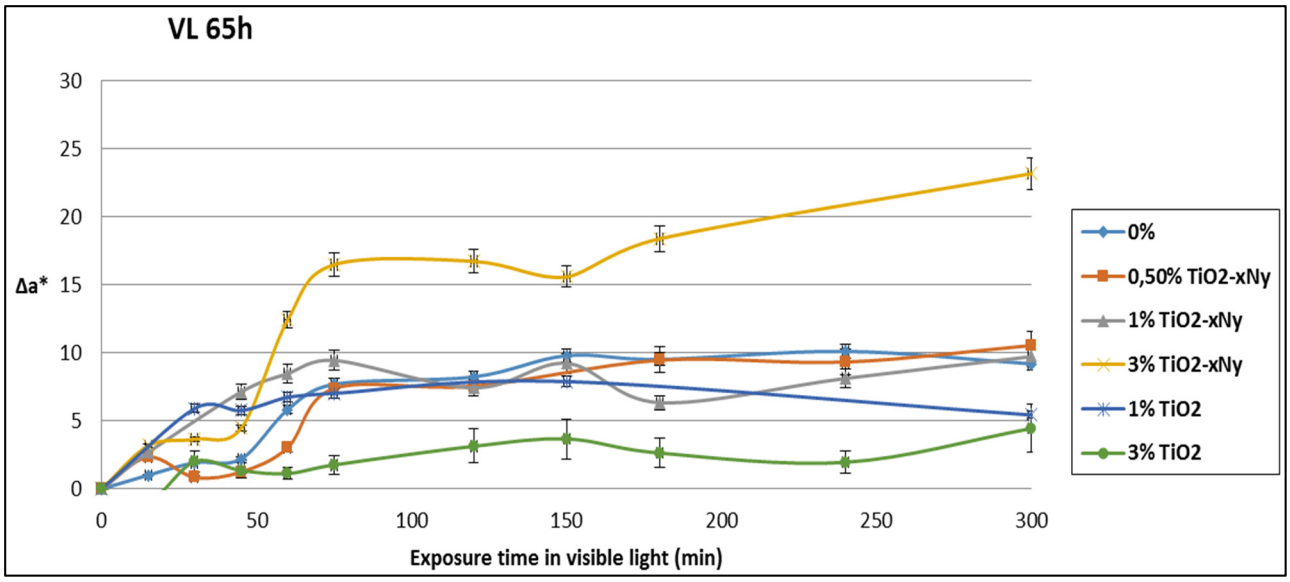

Figure 5. Change in Δa^* during 5 h exposure to visible light with different addition percentages of $TiO_{2-x}N_y$ and TiO_2 for samples at 65 h of curing age.

Table 2. Standard deviation of samples with $TiO_{2-x}N_y$ in visible light.

Sample	% $TiO_{2-x}N_y$	L_0^*	a_0^*	b_0^*	L^*	a^*	b^*	ΔE	Variance a^*	Standard Deviation a^*
A_1	0	64.60	67.90	−35.17	80.33	58.71	−23.45	21.65	**0.000648**	**0.025455844**
A_2	0	68.84	69.94	−34.39	79.30	58.75	−22.75	19.24		
B_1	0.5	66.15	68.09	−35.43	81.79	57.55	−23.25	22.47	**5.5677845**	**2.359615329**
B_2	0.5	63.429	67.77	−33.7	79.59	54.213	−23.807	23.3		
B_1	1	67.405	49.809	−32.181	82.102	40.085	−14.098	25.24	**3.1777205**	**1.782616195**
B_2	1	69.915	50.46	−34.871	81.559	42.606	−16.775	22.905		
C_1	3	75.51	63.207	−31.92	83.163	40.038	−14.787	29.81	**0.2628125**	**0.512652416**
C_2	3	74.202	60.164	−32.178	77.017	40.763	−15.653	25.63		

Table 3. Standard deviation of samples with TiO_2 in visible light.

Sample	% TiO_2	L_0*	a_0*	b_0*	L*	a*	b*	ΔE	Variance a*	Standard Deviation a*
D_1	1	77.189	56.42	−33,115	88.339	50.988	−21.831	16.76	**0.006728**	**0.082024387**
D_2	1	74.513	57.788	−33,322	64.162	51.104	−21.06	17.38		
E_1	3	71.784	63.023	−37,562	70.132	58.578	−26.049	12.45	**8.602952**	**2.933078928**
E_2	3	73.469	63.501	−37,292	79.723	62.726	−27.142	11.94		

The tables above show some data of the samples evaluated in visible light. Standard deviation was calculated for a* coordinate in all the samples. At the same time, the ΔE was calculated. This represents the change in color that is defined as the difference between two points of values, in the Euclidean sense [20]. The higher the ΔE, the higher the change in color. ΔE is defined as:

$$\Delta E = \sqrt{(L_0^* - L_t^*)^2 + (a_0^* - a_t^*)^2 + (b_0^* - b_t^*)^2} \quad (8)$$

It is noteworthy that the band gap of TiO_2 corresponds to 3.2 eV per atom; therefore, to do the electronic jump from the valence band to the conduction band and generate redox species, it is necessary to induce the particles and a suitable stimulus in terms of light or energy photons located in the range of near ultraviolet (UVA). On the other side, the inclusion of nitrogen atoms in the structure of TiO_2, as mentioned above, causes a decrease in the band gap, achieving the previously stated electronic jump more easily. In this form, it is possible to have photocatalytic activity in wavelengths between 400 nm and 700 nm. This can be observed in specimens with 3% of $TiO_{2-x}N_y$ that showed a percentage above the others. Samples with a low percentage of $TiO_{2-x}N_y$ showed low photoactivity, possibly due to the characteristics of the nanoparticles used. It is possible that commercial nano-$TiO_{2-x}N_y$ has a low doping degree of nitrogen and, for this reason, it requires high percentages in order to improve the efficiency. These results show that it is possible to obtain cements photoactivated with a self-cleaning property in visible light, but it is necessary to evaluate them in other conditions.

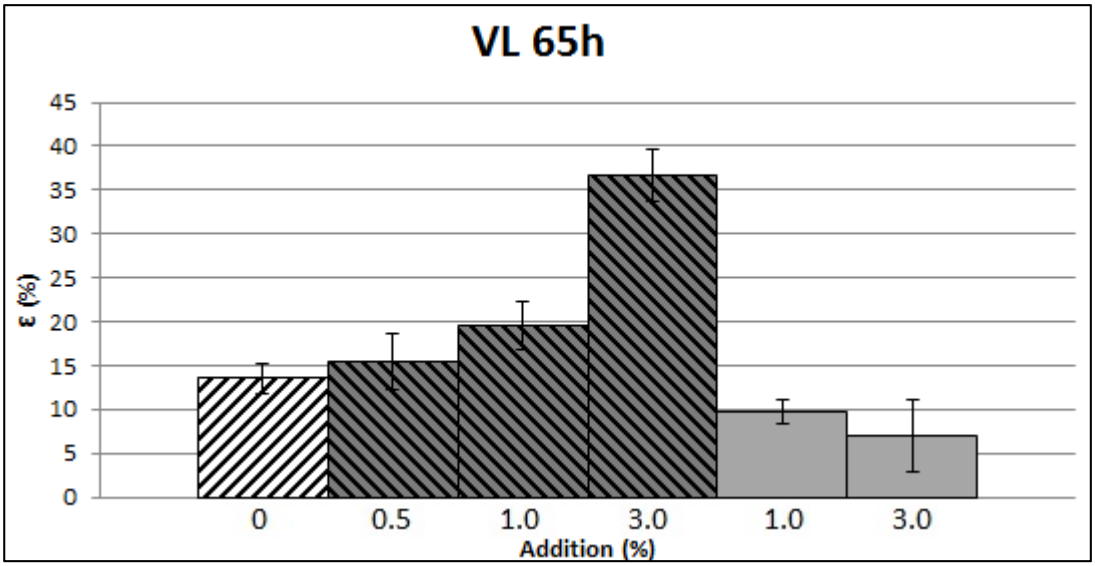

Figure 6. Photocatalytic efficiency Coefficient (ε) for samples in Visible light with 1%, 3% $TiO_{2-x}N_y$ and 1%, 3% TiO_2 for samples at 65 h of curing age, ▨ control sample, ▩ $TiO_{2-x}N_y$, ▭ TiO_2. Errors bars are standard deviation.

4. Conclusions

The addition of $TiO_{2-x}N_y$ nanoparticles to cement gives the ability to abate organic compounds present on the cementitious matrix, thus giving cement the attribute of being able to destroy contaminants by irradiating them with visible and UV light. With the best performance, samples with 3% $TiO_{2-x}N_y$ showed a similar behavior to 3% TiO_2 samples under UV irradiation. On the other hand, the results under visible light were different; the samples with TiO_2 did not show photocatalytic activity. In turn, these samples obtained a minimal abatement of dye by reactions of photolysis or thermolysis, and, possibly, a shielding effect was observed that prevented the photonic absorption in the pigment. In addition, the specimens with 3% of $TiO_{2-x}N_y$ obtained the highest photoactivity, and the samples with 1% of $TiO_{2-x}N_y$ showed a similar behavior to the control samples.

Cements with added $TiO_{2-x}N_y$ nanoparticles show potential to be applicable in the construction of photocatalytic structure, which can take advantage of much of the solar spectrum and artificial lighting for the degradation of organic pollutants present in these.

Acknowledgments

This work was supported by the "National program of projects for strengthening research, development and innovation in graduate 2014–2015" of the National University of Colombia. The authors would like to thank the university, but especially the Materials Characterization Laboratory of the faculty of mines from the National University of Colombia campus.

Author Contributions

Juan D. Cohen and Jorge I. Tobón have conceived and designed the experiments; Juan D. Cohen performed the experiments; G. Sierra-Gallego, Jorge I. Tobón and Juan D. Cohen analyzed the data. G. Sierra-Gallego and Jorge I. Tobón have contributed with the reagents and analysis tools. Juan D. Cohen wrote the paper.

Conflicts of Interest

The authors declare no conflict of interest.

References

1. Nochaiya, T.; Chaipanich, A. Behavior of multi-walled carbon nanotubes on the porosity and microstructure of cement-based materials. *Appl. Surf. Sci.* **2011**, *257*, 1941–1945.
2. Tobón, J.I.; Payá, J.J.; Borrachero, M.V.; Restrepo, O.J. Mineralogical evolution of Portland cement blended with sílica nanoparticles and its effect on mechanical strength. *Constr. Build. Mater.* **2012**, *36*, 736–742.
3. Oltulu, M.; Azahin, R. Single and combined effects of nano-SiO_2, nano-Al_2O_3 and nano-Fe_2O_3 powders on compressive strength and capillary permeability of cement mortar containing silica fume. *Mater. Sci. Eng. A* **2011**, *528*, 7012–7019.

4. Italcementi, S.P.A. Titanium Dioxide Based Photocatalytic Composites and Derived Products on a Metakaolin Support. U.S. Patent 8092586 B2, 10 January 2009.
5. Domènech, X.; Jardim, W.F.; Litter, M.I. Procesos avanzados de oxidación para la eliminación de contaminantes. In *Eliminación de contaminantes por fotocatálisis heterogénea*; Blesa, M.; Ed.; CYTED (Ibero-American Science and Technology for Sustainable Development): La Plata, Argentina, 2002; pp. 3–26.
6. Candal, R.; Bilmes, S.; Blesa, M. Semiconductores con actividad fotocatalítica. In *Eliminación de contaminantes por fotocatálisis heterogénea*; Blesa, M., Ed.; CYTED (Ibero-American Science and Technology for Sustainable Development): La Plata, Argentina 2002, pp. 79–101.
7. Cárdenas, C.; Tobón, J.; García, C.; Vila, J. Functionalized building materials: Photocatalytic abatement of NO_x by cement pastes blended with TiO_2 nanoparticles. *Constr. Build. Mater.* **2012**, *36*, 820–825.
8. Strini, A.; Cassese, S.; Schiavi, L. Measurement of benzene, toluene, ethylbenzene and *o*-xylene gas phase photodegradation by titanium dioxide dispersed in cementitious materials using a mixed flow reactor. *Appl. Catal. B Environ.* **2005**, *61*, 90–97.
9. Diamanti, M.V.; Del Curto, B.; Ormellese, M.; Pedeferri, M.P. Photocatalytic and self-cleaning activity of colored mortars containing TiO_2. *Constr. Build. Mater.* **2013**, *46*, 167–174.
10. Ruot, B.; Plassais, A.; Olive, F.; Guillot, L.; Bonafous, L. TiO_2-containing cement pastes and mortars: Measurements of the photocatalytic efficiency using a rhodamine B-based colourimetric test. *Sol. Energy* **2009**, *83*, 1794–1801.
11. Cárdenas, C.; Tobón, J.; García, C. Photocatalytic properties evaluation of Portland white cement added with TiO_2-Nanoparticles. *Rev. LatinAm. Metal. Mat.* **2013**, *33*, 316–322.
12. Asahi, R.; Morikawa, T.; Ohwaki, T.; Aoki, K.; Taga, Y. Visible-light photocatalysis in nitrogen-doped titanium oxides. *Science* **2001**, *293*, 269–271.
13. Di Valentin, C.; Finazzi, E.; Pacchioni, G.; Selloni, A.; Livraghi, S.; Paganini, M.C.; Giamello, E. N-doped TiO_2: Theory and experiment. *Chem. Phys.* **2007**, *339*, 44–56.
14. Kitano, M.; Funatsu, K.; Matsuoka, M.; Ueshima, M.; Anpo, M. Preparation of nitrogen-substituted TiO_2 thin film photo catalysts by the radio frequency magnetron sputtering deposition method and their photo catalytic reactivity under visible light irradiation. *J. Phys. Chem. B* **2006**, *110*, 25266–25272.
15. Hong, Y.C.; Bang, C.U.; Shin, D.H.; Uhm, H.S. Band gap narrowing of TiO_2 by nitrogen doping in atmospheric microwave plasma. *Chem. Phys. Lett.* **2005**, *413*, 454–457.
16. Yin, S.; Aita, Y.; Komatsu, M.; Wang, J.; Tanga, Q.; Satoa, T. Synthesis of excellent visible-light responsive $TiO_{2-x}N_y$ photocatalyst by a homogeneous precipitation-solvothermal process. *J. Mater. Chem.* **2005**, *15*, 674–682.
17. Amadelli, R.; Samiolo, L.; Borsa, M.; Bellardita, M.; Palmisano, L. N-TiO_2 Photocatalysts highly active under visible irradiation for NO_x abatement and 2-propanol oxidation. *Catal. Today* **2013**, *206*, 19–25.
18. Yousefi, A.; Allahverdi, A.; Hejazi, P. Effective dispersion of nano-TiO_2 powder for enhancement of photocatalytic properties in cement mixes. *Constr. Build. Mater.* **2013**, *41*, 224–230.
19. UNI 11259 Determinazione dell'attività fotocatalitica di leganti idraulici: Metodo della rodammina; UNI (Ente italiano di normazione): Milano, Italy, 2008.

20. Billmeyer, F.W.; Saltzman, M. *Principles of Color Technology*, 2nd ed.; John Wiley & Sons: New York, NY, USA, 1966; pp. 31–52.
21. Chen, F.; Zhao, J.; Hidaka, H. Highly selective deethylation of rhodamine B: Adsorption and photooxidation pathways of the dye on the TiO_2/SiO_2 composite photocatalyst. *Int. J. Photoenergy* **2003**, *5*, 209–217.
22. Colón, G.; Murcia López, S.; Hidalgo, M.C.; Navío, J.A. Sunlight highly photoactive Bi_2WO_6–TiO_2 heterostructures for rhodamine B degradation. *Chem. Commun.* **2010**, *46*, 4809–4811.
23. Chen, J.; Kou, S.; Poon, C. Photocatalytic cement-based materials: Comparison of nitrogen oxides and toluene removal potentials and evaluation of self-cleaning performance. *Build. Environ.* **2011**, *46*, 1827–1833.
24. Chen, J.; Kou, S.; Poon, C. Hydration and properties of nano-TiO_2 blended cement composites. *Cem. Concr. Compos.* **2012**, *34*, 642–649.